

Supplementary information

Supplementary figures

Figure S1 Level of mycDET1 protein in DET1 OE-1, OE-2 and OE-3 transgenic lines.

Total protein extract from wild type Col0, *det1-1* mutant and DET1 OE lines were analyzed by immunoblot with anti-DET1 and anti-RbCL antibodies as loading control. **(A)** Level of mycDET1 protein in DET1 OE-1, OE-2 and OE-3 transgenic lines. **(B)** Level of mycDET1 protein in DET1 OE-3 transgenic line. A two- to ten-fold dilution of DET1 OE-3 extract allows comparing endogenous DET1 and mycDET1 levels.

Figure S2 The mycDET1 fusion protein is functional *in planta*. The DET1 OE-3 transgene was introduced in the *det1-1* mutant by crossing, and phenotypes of homozygous progeny seedlings from the F3 were recorded. **(A)** Representative phenotypes of 2-week-old seedlings grown under normal light conditions. **(B)** Representative skotomorphogenic phenotypes of 5-day-old seedlings. **(C)** Hypocotyl length of 5-day-old seedlings grown in darkness or under normal light conditions. Error bars represent standard deviations from three replicates with $n > 20$ per replicate. Bar indicates 5 mm.

Figure S3 In contrast to *det1-1* mutant, DET1-overexpressing plants display normal levels of photolyase mRNAs and of UV-absorbing compounds. **(A)** Photolyase mRNA levels. Quantitative RT-PCR analysis of *PHRI* (black bars) and *UVR3* (white bars) mRNA levels was performed on 5-day-old seedlings. For each gene, the mRNA level was normalized relative to At4g29130 and At5g13440 house-keeping genes and to wild-type level arbitrarily set to 1. Error bars represent standard deviations from three replicates. **(B)** Representative profile of UV-absorbing compounds from wild-type, DET1 OE-3 line and *det1-1* mutant seedlings. Soluble pigments were methanol-extracted from similar amounts of fresh material and the absorbance was scanned from 200 to 450 nm as in Castells et al (2010).

Figure S4 DET1 interaction with Arabidopsis DDB1A and DDB1B proteins visualized by bimolecular fluorescence complementation (BiFC). Different combinations of plasmids expressing YFP N-terminal (YN) and YFP C-terminal (YC) parts fused to DET1, DDB1A, DDB1B and DDB2 proteins were used to co-transform mustard etiolated seedlings. A third construct expressing CFP-CPRF2 translational fusion targeted to the nucleus was also co-bombarded and used as a control to identify transformed cells. Images using CFP and YFP filters are shown (right panels and middle panels, respectively), as well as differential interference contrast (DIC, left panels). Specificity of signal following YFP-reconstitution was confirmed by absence of signal in transformed nuclei with YN-DET1 or YC-DDB2 co-bombarded with the respective empty YC or YN vectors.

Figure S5 OE-3 plants are deficient for synthesis-dependent repair of UV-damaged DNA. Cell extracts from wild-type and DET1 OE-3 plants were incubated for 0 or 2h with UV-C damaged (+UV) and undamaged control plasmid (-UV) in the presence of DIG-dUTP to monitor synthesis DNA repair. Similar amounts of input protein extracts added (20 μ g) were run in parallel on a 10% SDS-PAGE and coomassie staining is shown as protein loading control.

Figure S6 Sensitivity to cisplatin. One-week-old *det1-1*, *ddb2-2*, DET1 OE-3 and wild-type plants were cultured in presence of 5 μ M of cisplatin. Relative weight was calculated relative to the corresponding untreated plants as in Molinier et al (2008). Ten plants were used per replicate and the experiment was performed in triplicate. Asterisks indicate t-test significant differences at $p \leq 0.05$ relative to wild-type control at same dose.

Figure S7 Analysis of DET1 protein content in overexpressing lines upon UV-C exposure. (A) Immunoblot analysis of DET1 and mycDET1 levels before (-) or 30 min after UV-C exposure (+). (B) Size-exclusion analysis of the DET1 OE-3 extracts from (A). The inset shows DET1 and mycDET1 input content in DET1 OE-3 seedlings harvested before (-UV) or 30 min after UV-C exposure (+UV). Arrows indicate elution of molecular-weight standards in the same conditions.

Figure S8 Point mutation within a WD40 WDxR conserved motif affects DDB2 function in DNA repair. (A) Schematic representation of Arabidopsis DDB2 protein. WD40 domains are represented by white boxes, and position of the R343H point mutation (DDB2 WDxH) in the WDxR motif is indicated. (B) UV-induced root growth inhibition. Four-day-old seedlings with the indicated genotypes were exposed to 900 J/m² of UV-C and immediately returned to normal light conditions. Relative root growth was determined 24h after irradiation by comparison with the respective non-irradiated control of the same genotype (100% root growth). Error bars represent standard deviations from three replicate experiments. Asterisks indicate t-test significant differences at $p \leq 0.05$ relative to wild-type controls at the same dose.

Figure S9 Genetic interactions between *det1-1* and *ddb2-2* alleles on relative root growth upon exposure to 900 J/m² of UV-C. The *det1-1* and *ddb2-2* mutants are in the Col-0 and Nossen backgrounds, respectively. Null segregants in the F3 progeny from the cross between *det1-1* and *ddb2-2* are included in the analysis (DET1DDB2). Asterisks indicate t-test significant differences at $p \leq 0.05$ relative to wild-type controls at the same dose.

Figure S10 The DDB2 complex size is stable upon UV-C exposure. Size-exclusion chromatography analysis of DDB2 complex in soluble protein extracts from wild-type (A) and DET1 OE-3 (B). Experiments were performed as in Figure 6C. Fifty μ l of fractions 2 to 18 were analyzed by immunoblot using DDB2 antibody. Arrows indicate elution of molecular-weight standards in the same conditions. The inset shows DDB2 protein content in input samples for (A) before chromatography separation.

Supplementary methods

Bimolecular Fluorescence Complementation

The DET1, DDB1A, DDB1B and DDB2 coding sequences were isolated by PCR and cloned into the pDONR207 Gateway vector. The resulting entry vectors were used to introduce these cDNAs sequences into the split YFP destination vectors by Gateway Scientific technology to obtain YN-DET1, YC-DDB1A, YC-DDB1B and YC-DDB2

constructs. YN-, YC- and 35S–CPRF2–CFP are described elsewhere (Stolpe et al, 2005). Negative controls with vectors bearing YN or YC either alone were carried out in every experiment to verify the specificity of the interactions. The different constructs were transformed into 3-days-old, dark-grown mustard seedlings by particle bombardment. Images were recorded 16 h after bombardment with a Nikon fluorescente-equipped microscope E800 equipped with a 40x water immersion optic by using CFP- and YFP-specific filters. Positive signals were recorded, and interactions were considered as negative when 10% or less CFP-expressing nuclei (n>20) had no significant YFP signal. Reciprocally, interactions were considered as positive when 90% or more CFP-expressing nuclei (n>20) also had a significant YFP signal.

Cisplatin and hydrogen peroxyde treatments

For treatment with Cisplatin and hydrogen peroxyde (H₂O₂), 7 to 10 day-old Arabidopsis seedlings were transferred into 24-well culture plates containing liquid MS medium with 0, 5 or 10 µM of Cisplatin (Sigma) or 0, 2.5 or 5 mM of H₂O₂ (Sigma). The use of different concentrations allowed us to check the linear range of the treatment. The relative weight was calculated: (weight treated/ weight untreated)×100 (±SEM) for the most representative concentration (here 5 µM Cisplatin and 2.5 mM H₂O₂). Eight plants were used per point, and experiments were performed in triplicates.

Supplementary Table 1. Oligonucleotides list.

Gene	AGI ID	Primer Name	Primer Sequence
Ubiquinol-cytochrome C reductase iron-sulfur subunit	At5g13440	At5g13440 F	ACAAGCCAATTTTGTGCTGAGC
		At5g13440 R	ACAACAGTCCGAGTGTCATGGT
Hexokinase1	At4g29130	AT4G29130F	GGCGTTTTCTGATAGCGAAAA
		AT4G29130R	ATGGATCAGGCATTGGAGCT
UV Repair Defective 3	At3g15620	UVR3-F1	TCCGGTTCTTGCTTGAGAGT
		UVR3-R1	CAAAGCAAAGCCTCTTCACC
Photolyase 1	At1g12370	UVR2-F2	GGGACTGACAGCAGATCCTC
		UVR2-R2	GGGTCACGACCATCAATCTC
DET1	At4g10180	DET1 E2 Fwd	CGAATCTCCCGATCACTGTT
		DET1 E2 Rev	AGACCGAAACGACGAGTTTG

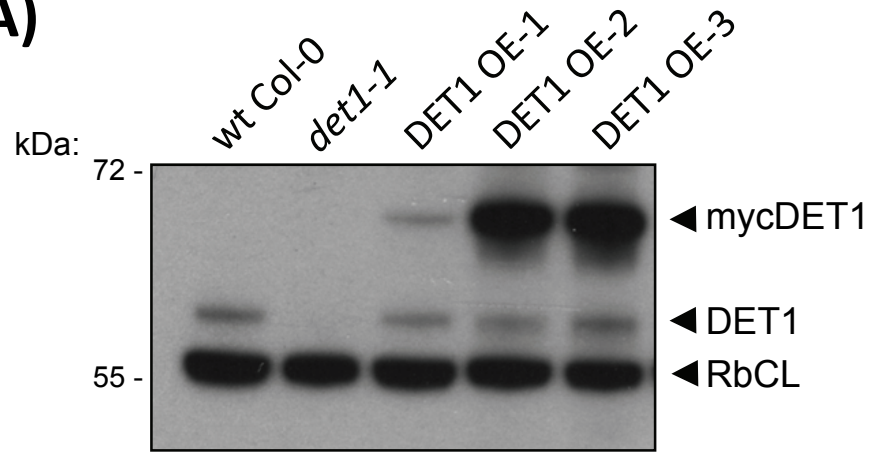
DDB2	At5g58760	DDB2_RT2_F	CAAAGCTGAATGGGACCCTA
		DDB2_RT2_R	ATTGTCCATTGCTTGCATCA

Supplementary references

Castells E, Molinier J, Drevensek S, Genschik P, Barneche F, Bowler C (2010) *det1-1*-induced UV-C hyposensitivity through UVR3 and PHR1 photolyase gene over-expression. *Plant J*: May 6, [Epub ahead of print]

Stolpe T, Susslin C, Marrocco K, Nick P, Kretsch T, Kircher S (2005) In planta analysis of protein-protein interactions related to light signaling by bimolecular fluorescence complementation. *Protoplasma* **226**: 137-146

(A)



(B)

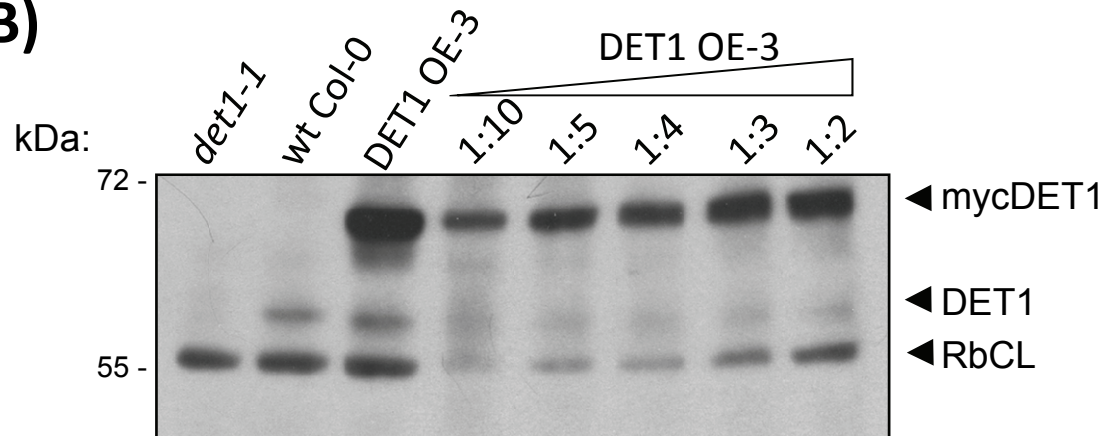


Figure S1

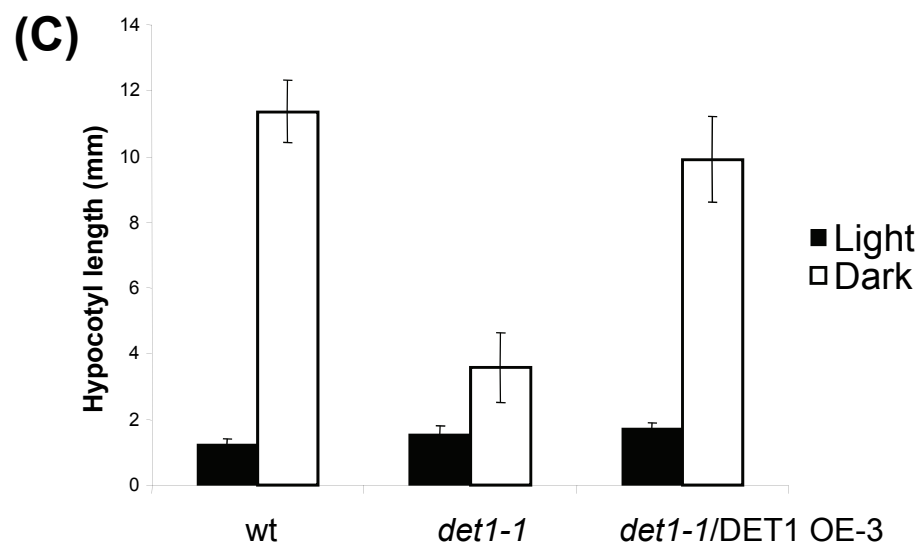
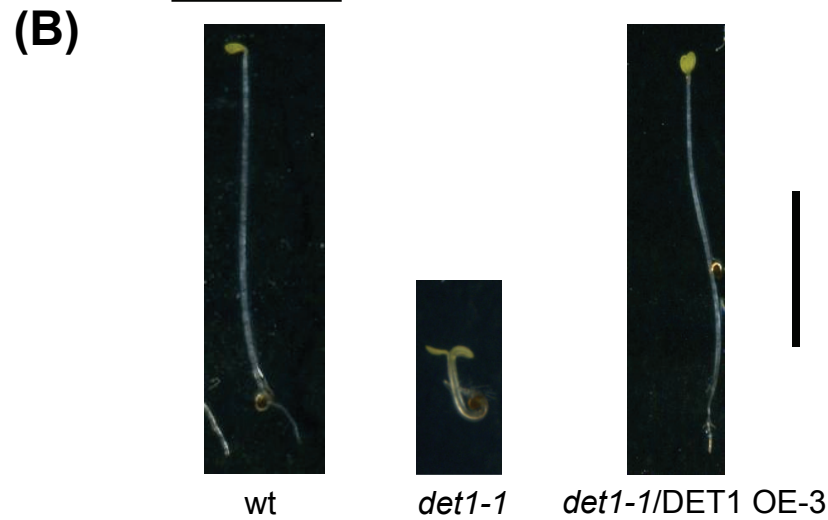
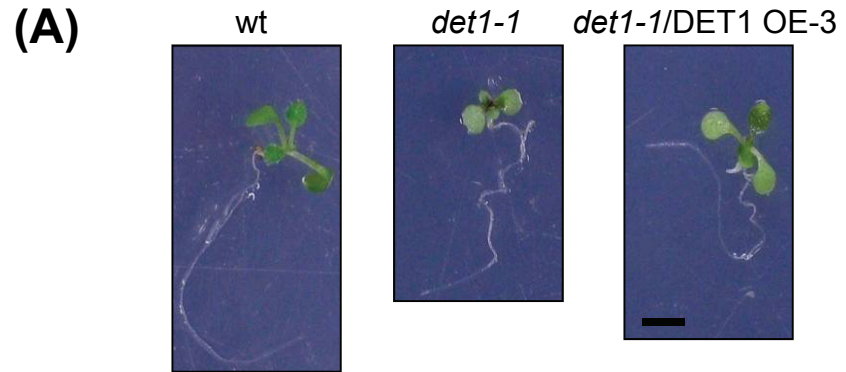


Figure S2

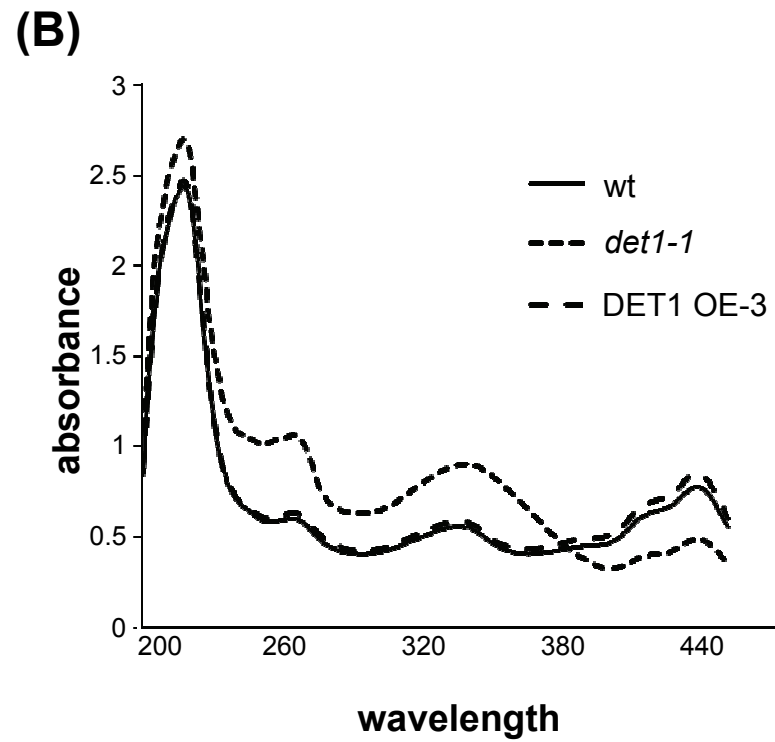
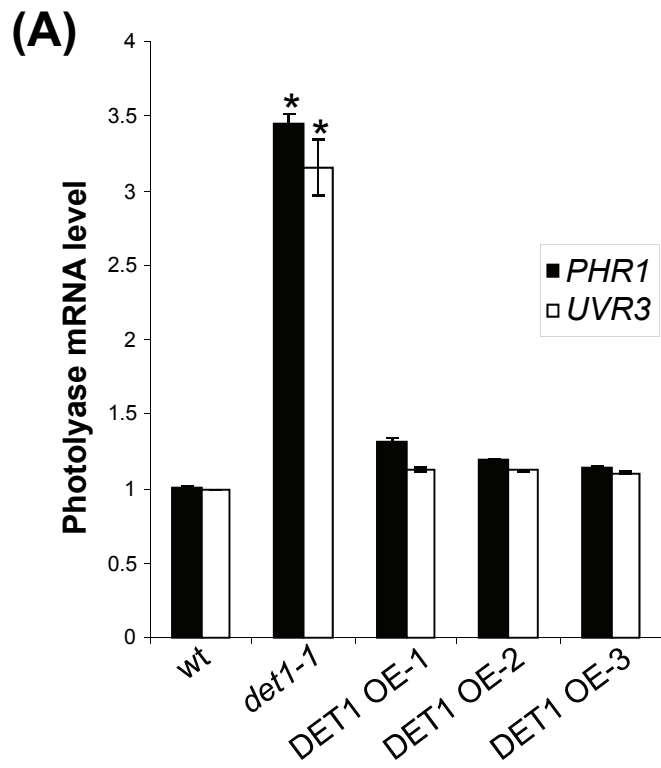


Figure S3

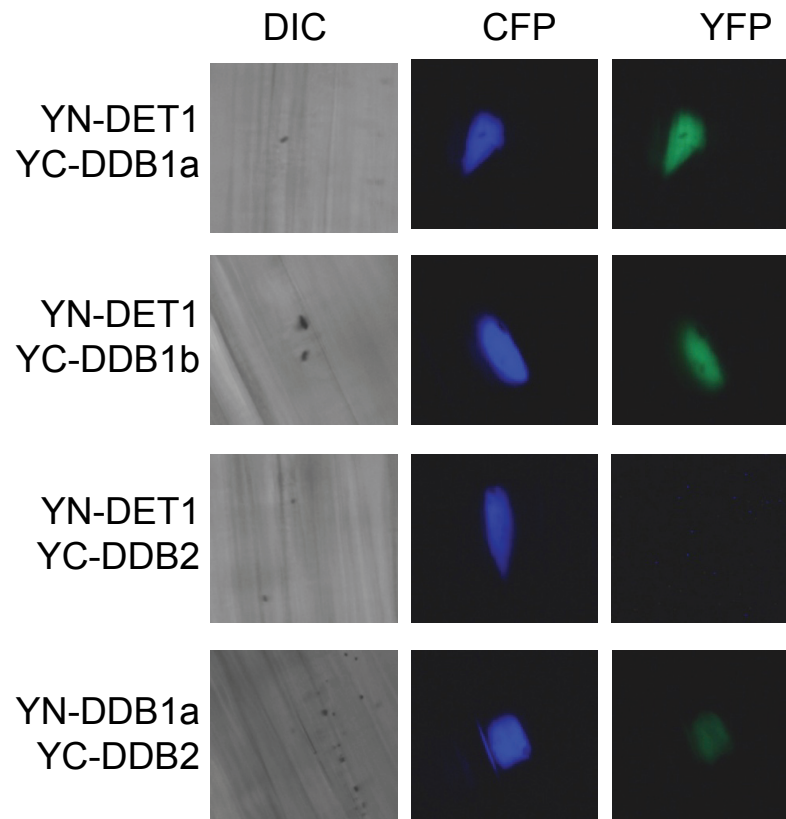


Figure S4

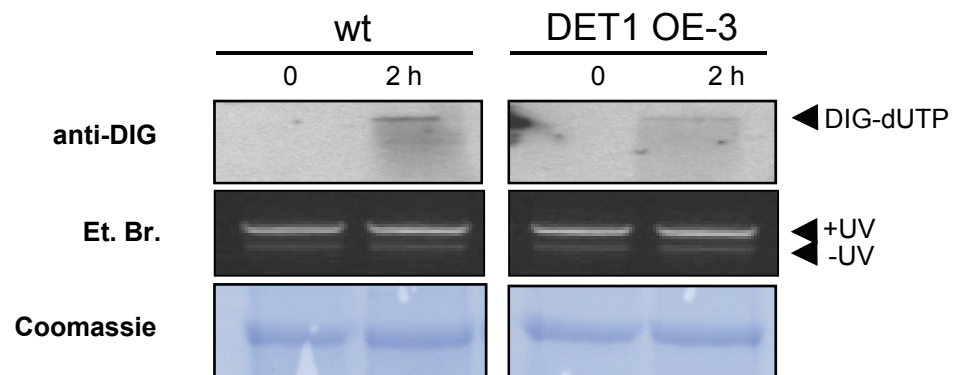


Figure S5

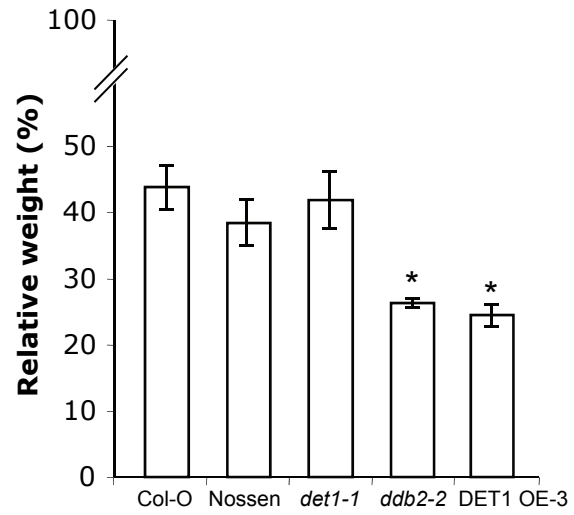
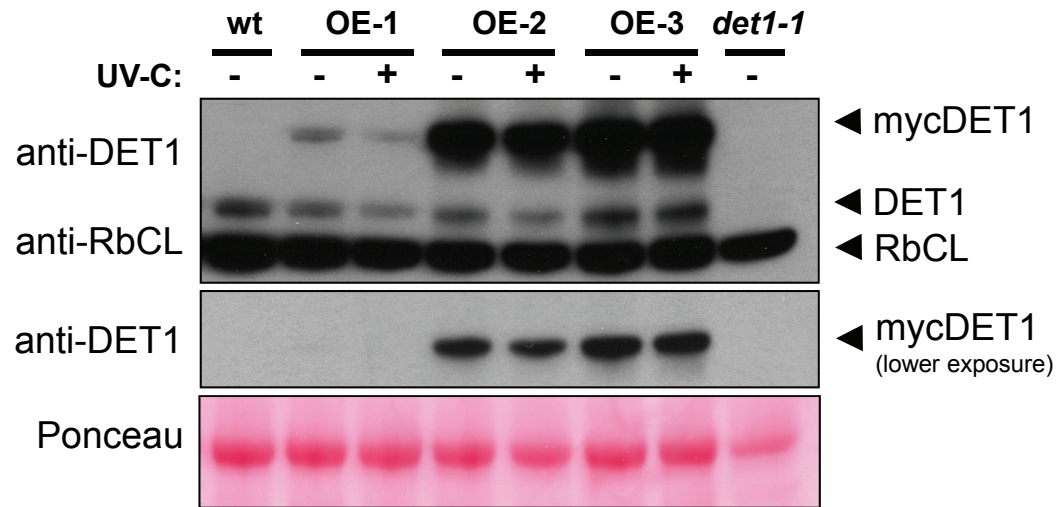


Figure S6

(A)



(B)

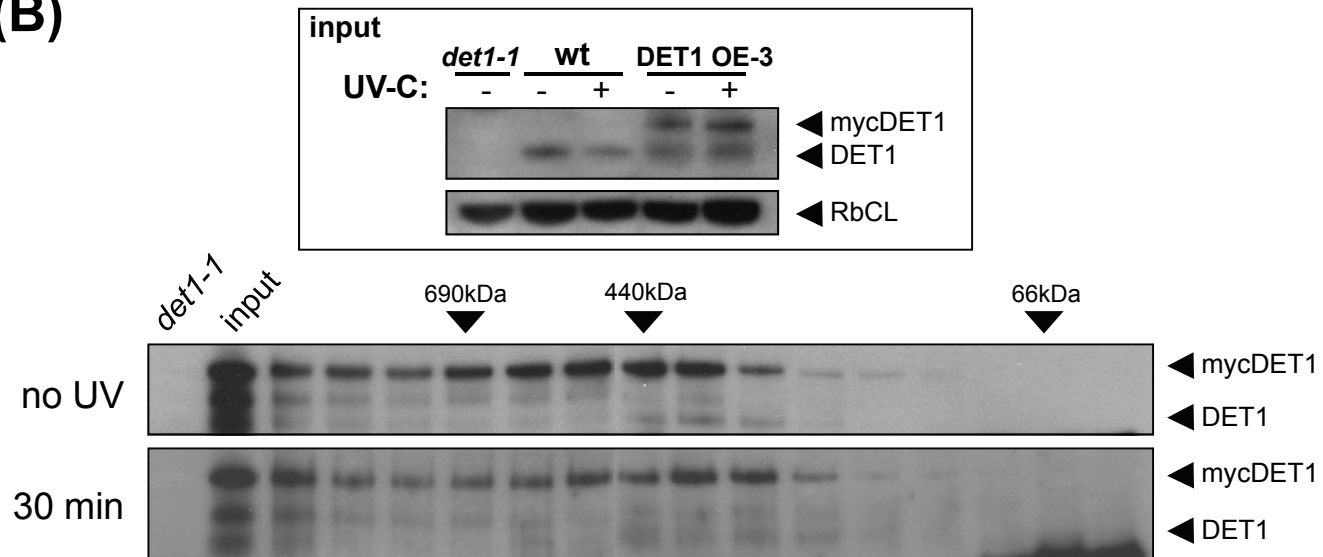
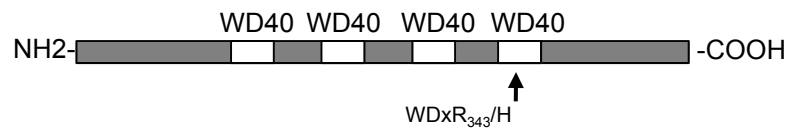


Figure S7

(A) Arabidopsis DDB2 protein



(B)

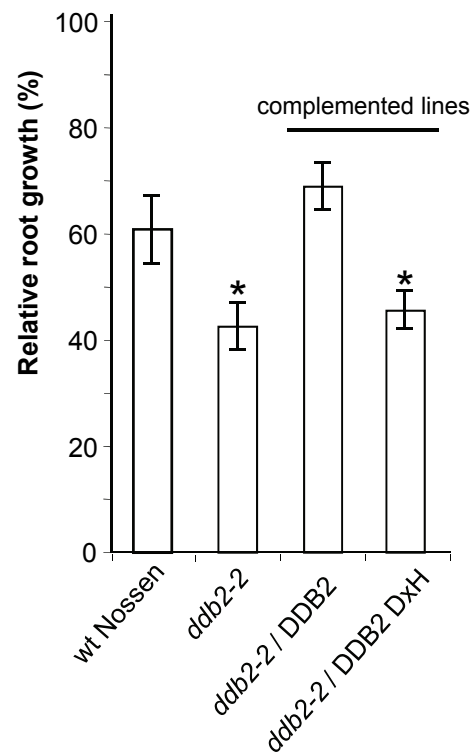


Figure S8

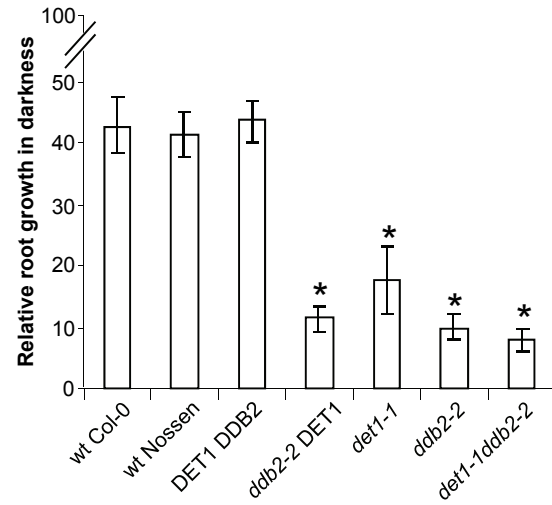
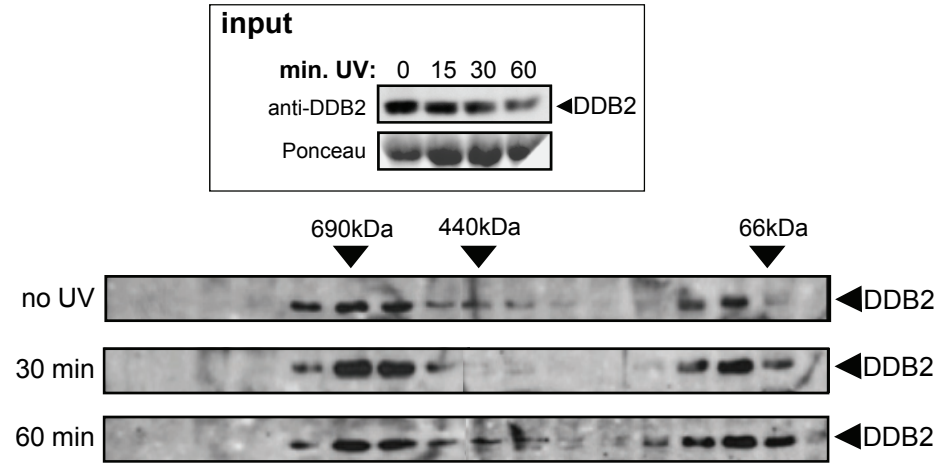


Figure S9

(A)



(B)

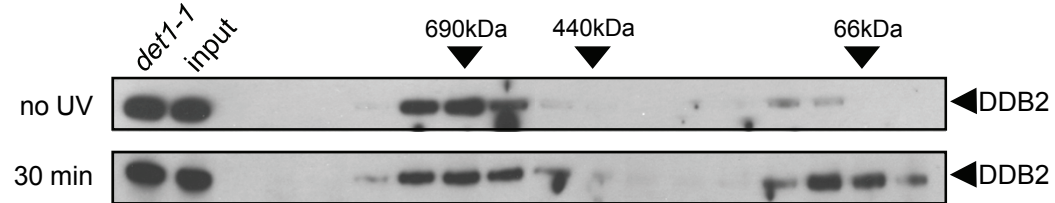


Figure S10